

Microwave-Assisted Neat Synthesis of a Ferrocene Appended Phenolphthalein Diyne: A Designed Synthetic Scaffold for Hg²⁺ Ion

Adwitiya Pal, Krishna Mohan Das, Bappaditya Goswami, and Arunabha Thakur*

Cite This: <https://dx.doi.org/10.1021/acs.inorgchem.0c01236>

Read Online

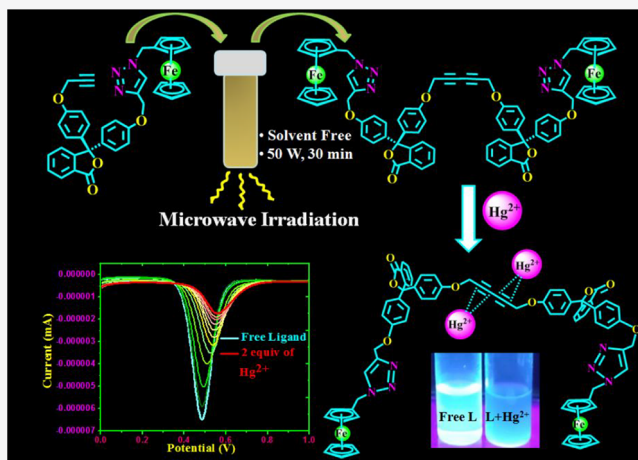
ACCESS |

Metrics & More

Article Recommendations

Supporting Information

ABSTRACT: A C₂-symmetric internally conjugated 1,3-dialkyne system **5**, containing phenolphthalein as a fluorophore and ferrocene as a redox moiety, has been synthesized via a microwave-assisted synthetic procedure. Compound **5** was synthesized by Cu-catalyzed Glaser–Hay coupling using a microwave reactor in neat condition for the first time. Compound **5** was found to be highly selective toward Fe³⁺, Cu²⁺, and Hg²⁺ ions via multichannels. Interestingly, Fe³⁺ and Cu²⁺ ions simply promote the oxidation of ferrocene unit to ferrocenium ion without binding to the receptor, whereas Hg²⁺ binds with the receptor **5** ($\Delta E_{1/2} = 71$ mV). The oxidation and binding phenomena were investigated by optical and electrochemical analyses. Furthermore, the binding site of Hg²⁺ ion with our designed probe was confirmed by ¹H, ¹³C NMR and IR titrations, which indicated that conjugated dialkyne unit interacts with Hg²⁺ ion by a favorable soft–soft interaction. Both receptor **5** and its metal complex, [5·2Hg²⁺], are stable in the physiological pH range (pH = 6–7) and thermally stable up to 78 °C. The experimental results of metal binding have been further supported by quantum chemical calculations (DFT), which explore the favorable geometry of the free ligand as well as its Hg²⁺ complex.



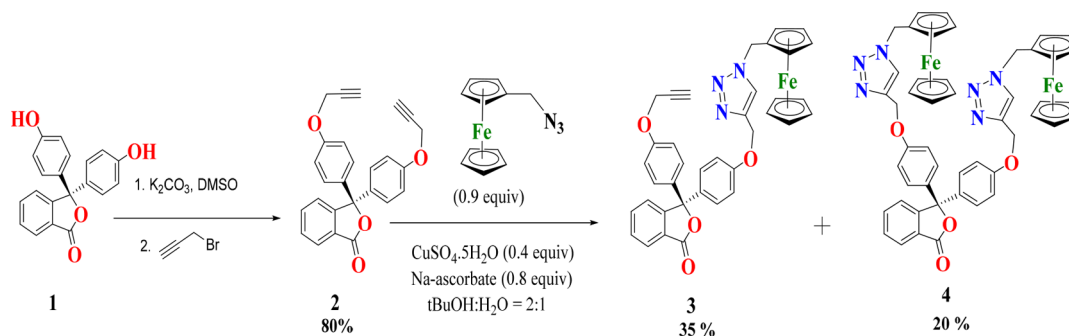
INTRODUCTION

1,3-Diynes represent a unique class of intermediates in organic synthesis and one of the most vital blocks in many natural products and functional materials.^{1,2} Conjugated alkynes are always advantageous because of their cylindrical electronic symmetry. The morphological beauty and beneficial properties of conjugated diynes have fascinated scientists to explore their scope of synthesis and utilization. The diyne moiety has been extensively utilized in many fields starting from nanoscience,³ liquid crystals,^{4–7} to antiviral activities,⁸ providing a strong motivation for modern research. Furthermore, they are used in optoelectronics,⁹ rotaxanes,^{10,11} catenanes,¹² pharmaceuticals,¹³ and polymer science.¹⁴ Mostly the diyne molecular systems have been developed so far by alkyne homocoupling and a few by heterocoupling¹⁵ using transition metal (e.g., Cu, Pd, Ni, and Au) catalysts. Such compounds can be prepared by the conventional Glaser coupling, Eglinton coupling, Hay coupling,^{16,17} as also by their modified versions.^{10–12} As an advancement of the synthetic methodology, microwave-assisted reactions in solvent phase¹⁸ and in solvent-free medium under thermal condition¹⁹ have also been explored for alkyne–alkyne coupling reactions. However, a microwave-assisted homogeneous synthesis of 1,3-diyne system in neat condition has not been explored earlier.

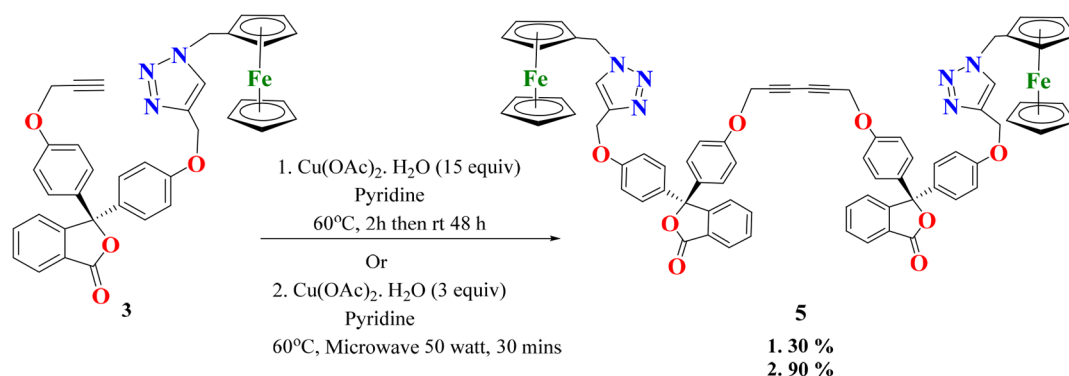
In spite of knowing for the last few decades that mercury has a strong propensity toward alkyne, very few examples are known where alkyne systems have been explored as structural building blocks for metal ions especially for mercury ion sensing.^{20,21} In this regard, a side-on coordination to Hg²⁺ ions by sterically accessible π -conjugation has been documented in the case of mercury–ethynyl interaction.^{22–24} A soft binding center (base) prefers to bind to a soft metal ion (acid) according to the HSAB principle.²⁵ Keeping this idea in mind, we have deliberately designed a structural motif, consisting of a 1,3-diyne system, which can interact and detect a soft Lewis acid, mercury. Mercury is one of the most investigated metal ions in the field of sensing owing to its extreme toxicity to living species.^{26–28} Mercury, in any form (e.g., elemental, inorganic, or organic forms) shows different kinds of toxicity. Hence, the design and development of any potential probe, capable of detecting the

Received: April 26, 2020

Scheme 1. Synthesis of Compounds 3 and 4



Scheme 2. Synthesis of Compound 5



released mercury, would be a step forward in making the environment safer for living species.

The design of metal ion sensors based on conjugated alkyne molecules may be the subject of growing interest because of its configurational and conformational rigidity.²⁹ Therefore, we have performed homocoupling of triazole-based ferrocene appended phenolphthalein alkyne in a dry medium to generate a dialkyne system that can be used as a potential metal ion sensor having multichannels. Fluorescence spectroscopy is a widely used and reliable technique for the detection of various metal ions in a precise and nondestructive manner.^{30–32} Phenolphthalein is taken as the fluorophore moiety so that fluorescence detection of the metal ion is possible, and ferrocene is appended to make the molecule redox active. Phenolphthalein is a popular pH indicator, but its scope of being used as the fluorophore in chemosensor molecules is not well-explored despite having a well-defined extended conjugation. In fact, it is not considered as an efficient fluorophore since it lacks structural rigidity due to the C–C single bond rotation.^{33,34} Hence, the easiest way to turn it into an effective fluorophore is by restricting its feasible C–C bond rotation. Interestingly, we have circumvented this issue, which is the root cause for being nonfluorescent, by functionalizing the hydroxyl groups by bulky substituents, and this modification has enabled us to convert it to a fluorescent derivative. On the other hand, the robustness in aerobic conditions, easy availability, economical affordability, ease of handling and storage, and most importantly its precise redox property make the ferrocene unit a topic of intensive research that has been well-explored.³⁵

In this work, we have developed a ferrocene-appended phenolphthalein diyne system by microwave synthesis in a neat condition. The present system, an easy-to-make optical and electrochemical sensor, displayed a high selectivity toward Hg^{2+}

ion. To the best of our knowledge, this is the first report of a conjugated dialkyne system for the detection of Hg^{2+} ion. A series of experiments and DFT calculations unravel the binding mode of the present probe with Hg^{2+} ion.

RESULTS AND DISCUSSION

Synthesis of Compound 5. In this work, we have developed a conjugated diyne bridged chromophore system by the homocoupling of two terminal alkynes with the pre-established protocol of the Eglinton coupling³⁶ with some advanced modifications. Microwave-assisted synthesis of the diyne system by the homocoupling of two terminal alkynes are reported in solvent phase;¹⁸ however, use of solvents, especially chlorinated solvents, make this strategy disadvantageous toward green synthesis. In this report, we have tried the microwave-assisted homocoupling of two terminal alkynes in neat condition at slightly elevated temperature with low catalyst loading to obtain the desired product. After successfully synthesizing the conjugated diyne bridged chromophore system via a modified method, we have investigated the metal-ion-sensing properties of the synthesized compound.

As shown in Schemes 1 and 2, phenolphthalein, 1, is converted into its dialkynyl derivative, 2, using K_2CO_3 as a base and propargyl bromide in DMSO at room temperature. Further, copper-catalyzed azide–alkyne [3 + 2] cycloaddition (CuAAC) reaction of 2 with mono(azidomethyl)ferrocene afforded compounds 3 and 4 in 35% and 20% yield, respectively. Conventional Eglinton coupling of compound 3 using $\text{Cu}(\text{OAc})_2 \cdot \text{H}_2\text{O}$ and pyridine as a base as well as a solvent afforded compound 5 in low yield (30%). As an advancement of conventional Glaser coupling, Eglinton coupling, Hay coupling, microwave-assisted heterogeneous as well as homogeneous homocoupling of terminal alkynes is reported either in alumina

Table 1. Optimization of Microwave-Assisted Eglinton Coupling Reaction in Our Specified Substrate

Sl. no.	equiv of 3	equiv of catalyst ^a	equiv of base/solvent	temperature (°C)	time (minutes)	% conversion	% yield
1	1	15	118 (5 mL)	60	10	20	6
2	1	15	118 (5 mL)	60	20	60	50
3	1	15	118 (5 mL)	60	30	100	90
4	1	1	118 (5 mL)	60	30	20	8
5	1	2	118 (5 mL)	60	30	65	49
6	1	3	118 (5 mL)	60	30	100	90
7	1	3	118 (5 mL)	25	30	10	5
8	1	3	118 (5 mL)	40	30	40	25
9	1	3.7	3 (19 μ L)	60	30	80	40

^aCatalyst is $\text{Cu}(\text{OAc})_2 \cdot \text{H}_2\text{O}$.

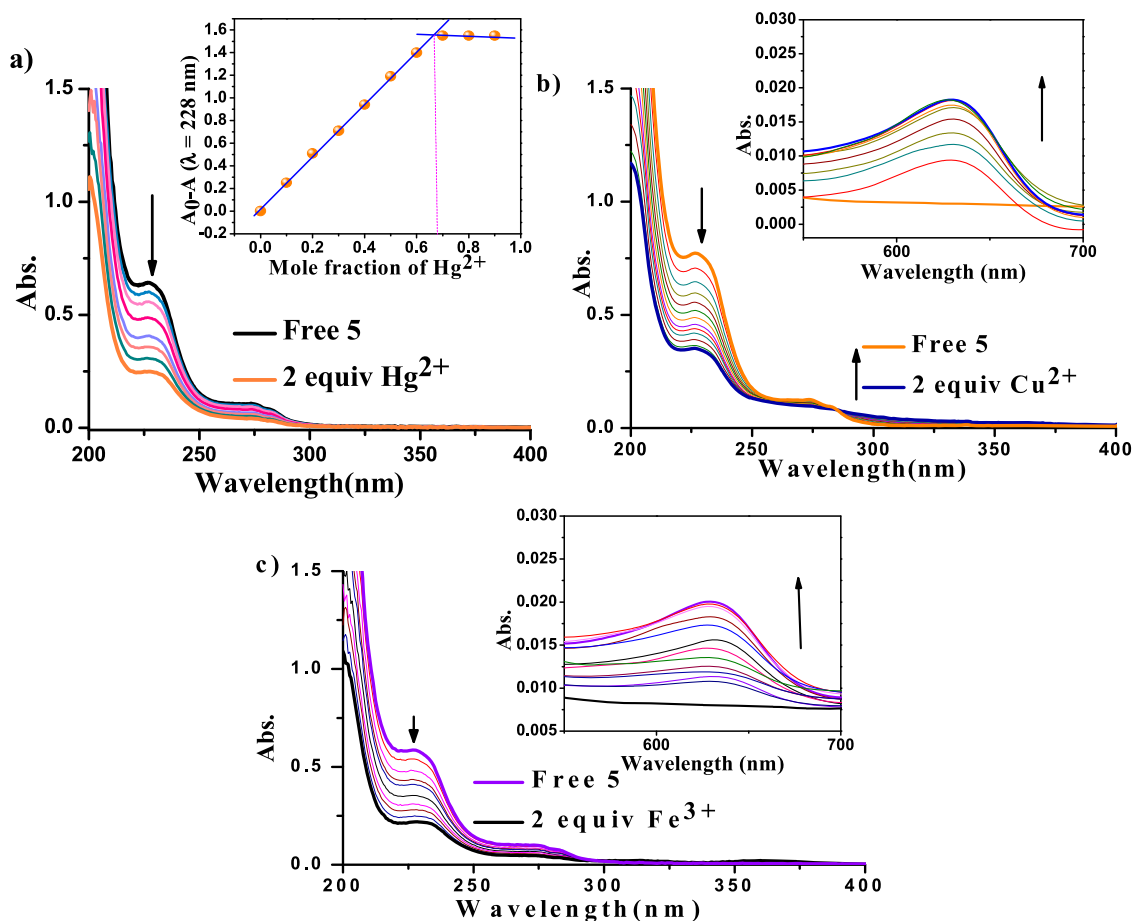


Figure 1. Absorption spectra of compound **5** (7.8×10^{-6} M) in CH_3CN solvent upon addition of up to (a) 2 equiv of Hg^{2+} (the inset shows the Job's plot); (b) 2 equiv of Cu^{2+} and (c) 2 equiv of Fe^{3+} at room temperature (the insets show the peak appearing due to oxidation of the ferrocene unit).

surface³⁷ or in solvent phase.¹⁸ Here, we wish to report a fast, solvent free microwave-assisted homogeneous Eglinton coupling of terminal alkynes.

As shown in Scheme 2 and Table 1, compound **5** can be achieved in 90% yield in just 30 min by employing microwave excitation to 50 W at 60 °C with low catalyst loading (3 equiv) compared with the conventional reaction method (15 equiv) mentioned earlier. For the further advancement of the reaction protocol, the reaction was performed in neat condition with only 3 equiv of pyridine (19 μ L) as a base and 3.7 equiv of $\text{Cu}(\text{OAc})_2 \cdot \text{H}_2\text{O}$, giving 80% conversion, under microwave irradiation. This is the first report of homogeneous Eglinton coupling in a solvent-free condition done under microwave irradiation and without any external solid support. All the synthesized compounds have

been characterized by ^1H and ^{13}C NMR spectroscopy, HRMS, and elemental analysis.

UV-vis Absorption Studies. The UV-vis spectra of compound **5** (7.8×10^{-6} M) with stepwise addition of solutions of Na^+ , K^+ , Fe^{2+} , Fe^{3+} , Cu^{2+} , Cu^+ , Hg^{2+} , Ag^+ , Ca^{2+} , Mg^{2+} , Mn^{2+} , Zn^{2+} , Pb^{2+} , Co^{2+} , Cr^{3+} , Al^{3+} ions (7.8×10^{-6} M) are recorded separately in CH_3CN solvent. From this experiment, we have observed that the receptor **5** selectively responded toward Hg^{2+} , Cu^{2+} , and Fe^{3+} ions (Figure S1) among all the aforementioned cations. The UV-vis spectra of compound **5** shows two absorption bands at $\lambda_{\text{max}} \sim 228$ nm ($\epsilon = 81\,907$ $\text{M}^{-1} \text{cm}^{-1}$) and 273 nm ($\epsilon = 13\,832$ $\text{M}^{-1} \text{cm}^{-1}$), corresponding to the excitation of the phenolphthalein moiety.³⁸ After the addition of each aliquot of the metal ions, the absorbance decreases, and it

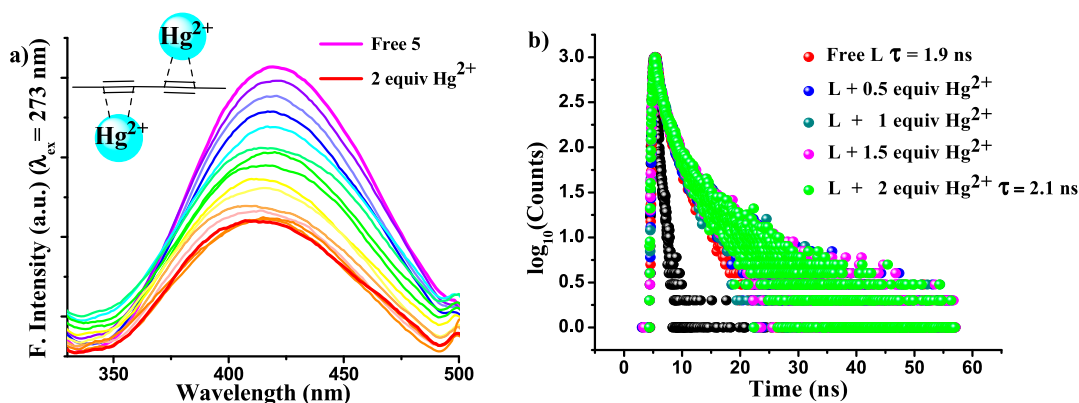


Figure 2. (a) Fluorescence emission titration spectra of compound **5** (6.62×10^{-6} M) upon addition of Hg^{2+} up to 2 equiv at room temperature; inset picture showing the probable interaction responsible for the quenching. (b) Mechanism of fluorescence quenching by fluorescence lifetime study of **5** with Hg^{2+} at room temperature: static quenching.

continues to fall gradually up to 2 equiv of each of Hg^{2+} , Cu^{2+} , and Fe^{3+} ions (Figure 1). On careful observation of the interaction of **5** with Cu^{2+} and Fe^{3+} ions (Figure 1b,c) inset, it is found that there occurs a small peak around 630 nm ($\epsilon = 7024 \text{ M}^{-1} \text{ cm}^{-1}$), corresponding to the oxidation of Fe(II) of ferrocene unit to Fe(III) of ferrocenium ion.³⁹ This peak diminishes gradually on addition of L-sodium ascorbate (LAS) as a reducing agent (Figure S2). This phenomenon clearly indicates that the oxidation–reduction of the ferrocene unit in **5** is reversible. Interestingly, no such peak at high wavelength was observed upon addition of Hg^{2+} ion. It may be concluded that the kind of interaction of receptor **5** toward Hg^{2+} ion is different from that toward Cu^{2+} and Fe^{3+} ions. Anticipating that the interaction can be of binding type, we have calculated the binding ratio of Hg^{2+} with probe **5** by binding assays using the method of continuous variation (Job's plot) (Figure 1a, inset), and it was found to be 2:1. Although our several attempts to obtain the mass spectra of the $[\text{5} \cdot 2\text{Hg}^{2+}]$ complex were unsuccessful, the binding ratio and composition were confirmed by elemental analysis of the isolated complex (vide supra).

Fluorescence Studies. To understand the properties of the synthesized molecule more clearly, fluorescence studies are indispensable as fluorescence spectroscopy acts as a supreme and precise analytical tool. We have modified the structure of phenolphthalein in order to make it a good fluorophore moiety and to obtain a considerable fluorescence emission intensity. Fluorescence spectra of **5** in the presence of Na^+ , K^+ , Fe^{2+} , Fe^{3+} , Cu^{2+} , Hg^{2+} , Ag^+ , Ca^{2+} , Mg^{2+} , Mn^{2+} , Zn^{2+} , Pb^{2+} , Co^{2+} , Cr^{3+} , Al^{3+} ions (as their perchlorate salts) and Cu^+ (as $[(\text{CH}_3\text{CN})_4\text{Cu}]\text{PF}_6$) are recorded separately in CH_3CN solution (6.62×10^{-6} M) with the excitation wavelength at 273 nm (low energy). Although excitation at 228 nm also produced similar results, we have avoided this high energy absorption band as the excitation wavelength. No significant change was observed in the emission spectra of **5** after addition of the metal ions except for Hg^{2+} , Cu^{2+} , and Fe^{3+} ions (Figure S3). As shown in Figure 2, the addition of Hg^{2+} ion up to 2 equiv exhibited a gradual diminishing fluorescence emission intensity with a small blue shift ($\Delta\lambda = 10$ nm) on excitation at 273 nm, and no further change was observed on addition of Hg^{2+} ion beyond 2 equiv. It is known that alkyne units have two perpendicular π -electron clouds,⁴⁰ and if two alkyne units are joined by a C–C single bond, that connecting single bond has slightly reduced bond length.^{41,42} Coordination of metal ion in this “triple–single–triple” bond unit can lead to a perturbation to the conjugation to

a slight extent and eventually may lead to a blue shift in fluorescence spectra.⁴³ It is evident from ^1H , ^{13}C NMR and IR spectral data that the alternate triple bonds are stable and prominent in our synthesized probe **5**. However, the change of the emission spectra ($\Delta\lambda = 10$ nm) on addition of Hg^{2+} ion led us to conclude that receptor **5** may bind Hg^{2+} ion through π -cloud via soft–soft interaction according to HSAB principle. The reversibility of this interaction of the probe **5** toward Hg^{2+} ion has also been investigated through the fluorescence spectroscopy by using aqueous solution of disodium EDTA (6.62×10^{-6} M) as the chelating agent (Figure S4). However, repeating the same experiment up to 2 equiv of Cu^{2+} and Fe^{3+} ions in a CH_3CN solution of compound **5**, fluorescence quenching, with no net shift of the intensity maxima, was observed (Figures S5, S6). Fe^{3+} and Cu^{2+} ions are known as efficient fluorescence quenchers^{44,45} may be due to their paramagnetic nature and Hg^{2+} ion led to the fluorescence quenching may be via ligand-to-metal charge transfer (LMCT), which was verified by TD-DFT calculations (vide supra). To get further insight into the quenching mechanism for Hg^{2+} , fluorescence lifetime measurement was performed. As shown in Figure 2b, lifetime of the undisturbed molecule (1.9 ns) remains almost constant even after addition of 2 equiv of Hg^{2+} ion (2.1 ns). Thus, the unchanged lifetime predicts the formation of a nonfluorescent complex in the ground-state,⁴⁶ indicating a static quenching phenomenon.

In order to understand the sensitivity of the probe **5** (6.62×10^{-6} M), we have performed the fluorescence titration using Hg^{2+} ion (6.62×10^{-6} M) in CH_3CN solution. A detectable change in fluorescence spectra was observed only in the presence of 0.015 equiv of Hg^{2+} ion; hence, the detection limit (DL) of Hg^{2+} with probe **5** is 9.9×10^{-8} M. Further, DL can also be precisely obtained via $3\sigma/S$ method,⁴⁷ where “ σ ” is the standard deviation of the blank and S is the slope of the calibration curve. A good linear relationship between the fluorescence intensity (data extracted from Figure 2a) and the concentration of Hg^{2+} was obtained (Figure S7). Interestingly, the limit of detection was obtained in the same order as that obtained from the above method. Further, binding constant value with Hg^{2+} ion have been calculated according to Stern–Volmer equation,⁴⁸ $I/I_0 = 1 + K[\text{Q}]$ (data plot Figure S8), where K is called the quenching constant, I is the intensity of fluorescence at the quencher concentration $[\text{Q}]$, and I_0 is its value without quencher. The binding constant value was found

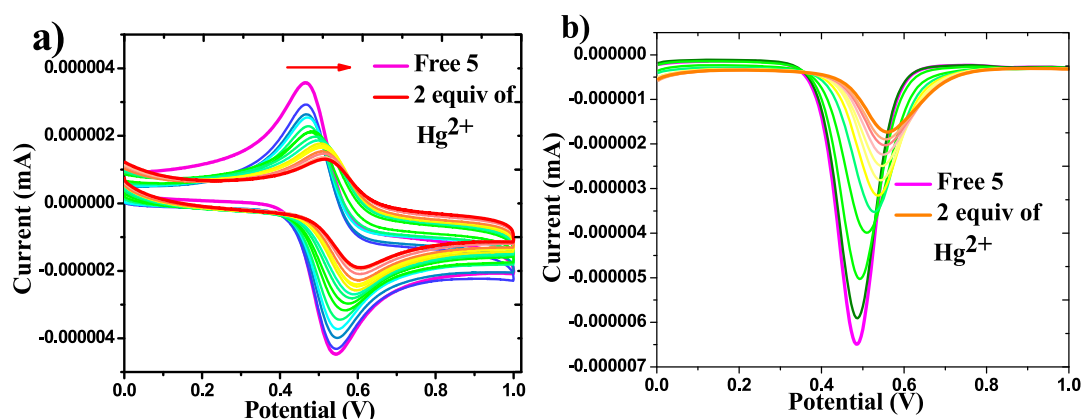


Figure 3. Evolution of (a) CV and (b) DPV of compound **5** (2.5×10^{-4} M) in CH_3CN solvent using $[(n\text{-Bu})_4\text{N}]\text{ClO}_4$ as supporting electrolyte when $\text{Hg}(\text{ClO}_4)_2$ is added up to 2 equiv at room temperature measured at a scan rate of 0.05 V s^{-1} .

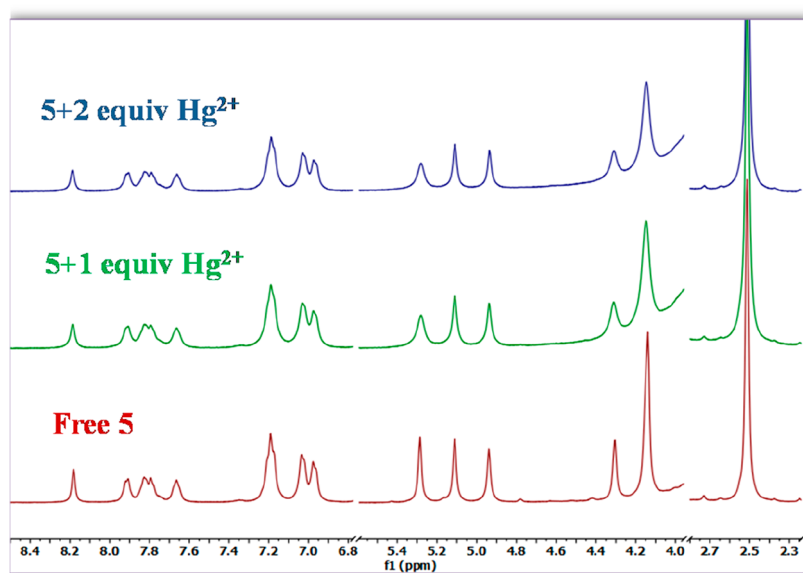


Figure 4. ^1H NMR titration of compound **5** with $\text{Hg}(\text{ClO}_4)_2$ in $d_6\text{-DMSO}$ solvent at room temperature.

to be $6.8 \times 10^3 \text{ M}^{-1}$, which indicates a weak interaction of Hg^{2+} with probe **5**.

Electrochemical Studies. The sole purpose of including ferrocene into the model of the probe is to carry out the various electrochemical studies of metal binding phenomenon because of its inherent reversible electrochemical nature.^{49,50} Among the various electrochemical studies known, cyclic voltammetry (CV) and differential pulse voltammetry (DPV) experiments are explored for the cation recognition mechanism study for the receptor **5**. A reversible one-electron oxidation process is observed for the receptor **5** (2.5×10^{-4} M) with a redox wave at $E_{1/2} = 0.504 \text{ V}$ due to oxidation of the Fe(II) of ferrocene to Fe(III) of ferrocenium ion and vice versa. The electrochemical behavior of compound **5** was investigated in the presence of Fe^{3+} , Cu^{2+} , and Hg^{2+} ions along with other metal ions (as their perchlorate salts) and Cu^+ as $[(\text{CH}_3\text{CN})_4\text{Cu}]\text{PF}_6$ in CH_3CN (2.5×10^{-4} M) solvent containing 0.1 M $[(n\text{-Bu})_4\text{N}]\text{ClO}_4$ as supporting electrolyte (Figure S9). No perturbation of the cyclic voltammogram (CV) was observed except in the case of Fe^{3+} , Cu^{2+} , and Hg^{2+} ions. As shown in the Figure 3a, stepwise addition of Hg^{2+} up to 2 equiv induced a significant shift of $\Delta E_{1/2} = 71 \text{ mV}$ of compound **5**, indicating the formation of a new

complex species, $[\text{5}\cdot 2\text{Hg}^{2+}]$. On the other hand, compound **5** did not exhibit any significant shift of $\Delta E_{1/2}$ upon addition of up to 2 equiv of Cu^{2+} and Fe^{3+} ions (Figures S10, S11), only the current got diminished with each aliquot of metal addition, indicating oxidation of ferrocene to ferrocenium ion.⁵¹ The DPV experiments also corroborated the same results as obtained from CV experiments (Figure 3b). A significant shift in potential of the complexed species was observed upon addition of Hg^{2+} ion and no net shift in potential, but rather current, was observed for the Fe^{3+} and Cu^{2+} ions (Figure S10). The responses of probe **5** toward the three metal ions remain unaffected by the presence of other metal ions.

^1H and ^{13}C NMR Titrations. From all the above experiments, it may be concluded that the present probe, **5**, binds with Hg^{2+} ion, but the binding site cannot be assigned unambiguously as **5** has multiple probable binding sites. Therefore, in order to find out the actual binding site, ^1H NMR titration was conducted in $d_6\text{-DMSO}$ at room temperature. Initially, ^1H NMR of compound **5** in $d_6\text{-DMSO}$ was recorded, and then 2 equiv of Hg^{2+} ion in $d_6\text{-DMSO}$ is added in two instalments consecutively (1 equiv + 1 equiv). Then the corresponding ^1H NMR spectra were recorded. Surprisingly, as shown in Figure 4, no net shift of

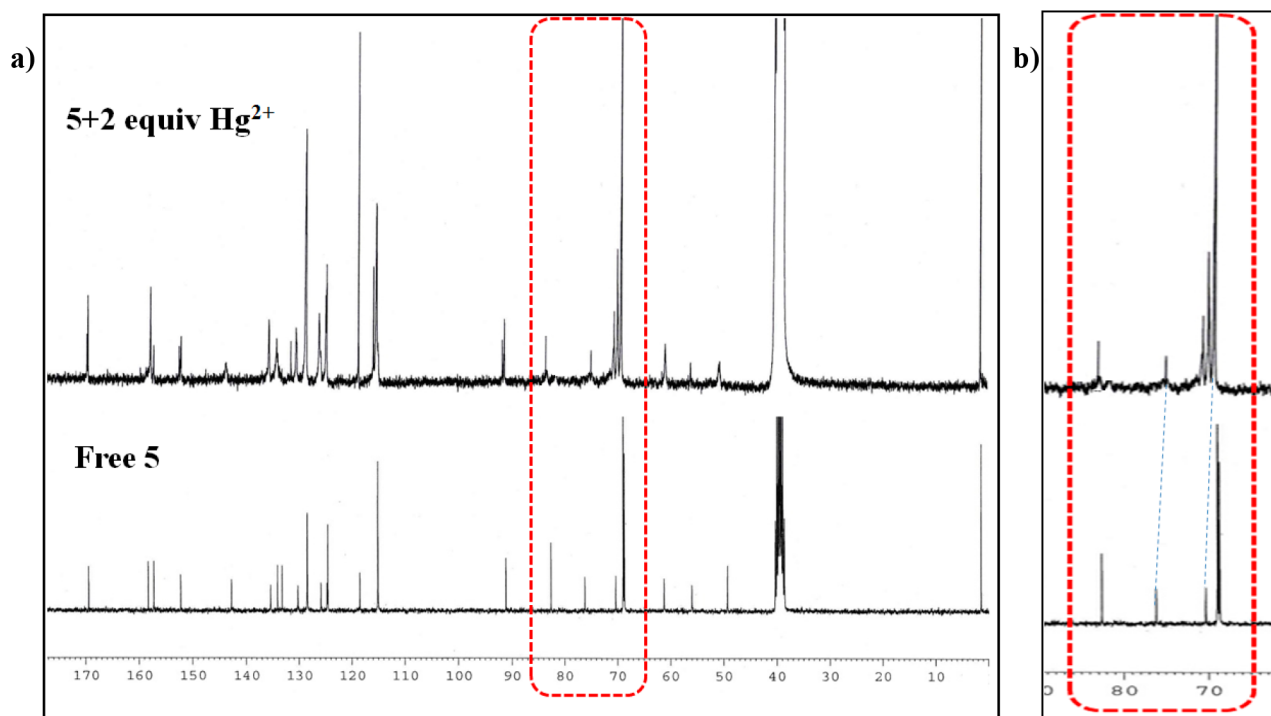


Figure 5. (a) ^{13}C NMR titration of compound **5** with 2 equiv of Hg^{2+} ion in d_6 -DMSO solvent at room temperature. (b) Selected part from 65 to 86 ppm.

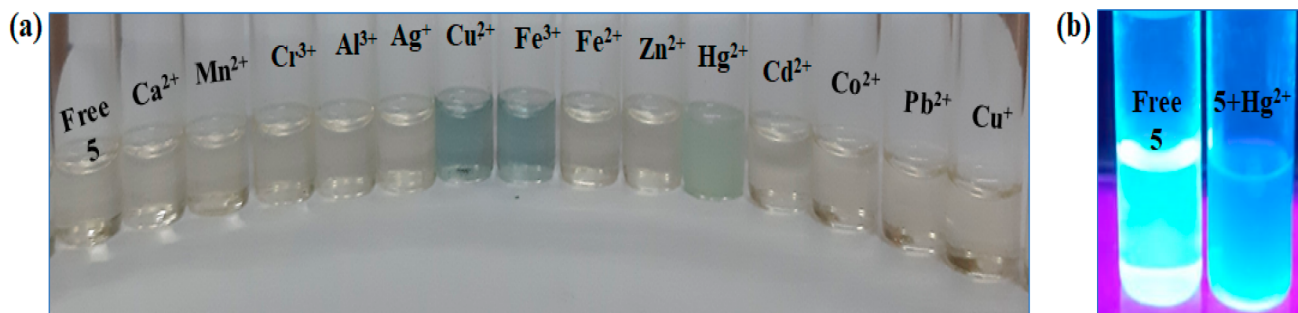


Figure 6. (a) Visual color changes observed for receptor **5** (10^{-4} M) in CH_3CN after addition of 1 equiv of several metal cations (10^{-4} M). (b) Irradiation of **5** and $[\mathbf{5}+\text{Hg}^{2+}]$ at 365 nm UV light under darkness in CH_3CN solvent.

any of the peaks (not even the peak at 8.18 ppm, corresponding to $-\text{CH}$ proton of triazole unit)⁵² in the ^1H NMR spectra was observed after the addition of 2 equiv of Hg^{2+} ion. It imparts the idea that the heteroatoms (O, N) present in the probe are probably not contributing to the binding of metal ion; had it been so, the corresponding adjacent H atoms in the ^1H spectra of the complexed moiety would have been shifted. Nevertheless, our original quest for determining the actual binding site unambiguously still remained unanswered.

In order to understand the binding site in detail, ^{13}C NMR titration was performed to shed some light on the binding mode for Hg^{2+} ion. As shown in Figure 5, addition of 2 equiv of Hg^{2+} into d_6 -DMSO solution of compound **5** led to the slight upfield shifts of the signals at 70.35 and 76.19 ppm. The signal corresponding to 76.19 ppm shifted upfield by 1.67 ppm, and another signal corresponding to 70.35 ppm was merged with the chemical shifts of ferrocene carbons. The signals at 70.35 and 76.19 ppm are attributed to the alkyne carbons, which were confirmed from $^1\text{H}-^{13}\text{C}$ HSQC spectral data (Figure S12) of **5** in d_6 -DMSO. All other signals corresponding to aromatic

carbons and triazole carbons show no obvious changes. This result clearly demonstrates that the conjugated alkyne part plays a vital role in interacting with the Hg^{2+} ion. The binding mode and this proposed mechanism has been further supported by IR titration and DFT studies (vide supra).

IR Titration. To further verify the proposed binding mode the IR titration was performed taking all the compounds in the solid state. Upon gradual addition of $\text{Hg}(\text{ClO}_4)_2$ up to 2 equiv, the peak at $\bar{\nu} = 2086\text{ cm}^{-1}$, corresponding to $\text{C}\equiv\text{C}$ stretching frequency, disappeared (Figure S13). This observation suggested the presence of some interaction between the dialkyne unit and metal ion, and this result agreed with our previous observation in ^{13}C NMR titration. Interestingly, no shifts were observed for the peak at $\bar{\nu} = 1752\text{ cm}^{-1}$, corresponding to the carbonyl moiety of the lactone ring, indicating no interaction with the Hg^{2+} ion. There is also a strong peak at $\bar{\nu} = 1085\text{ cm}^{-1}$, corresponding to the $\text{Cl}-\text{O}$ stretching frequency⁵³ of the ClO_4 unit, which results because of the inclusion of $\text{Hg}(\text{ClO}_4)_2$ unit in **5**. Therefore, combining all the results from NMR and IR

titration, it can be concluded that the plausible binding mode of Hg^{2+} ions is the conjugated dialkyne unit in probe **5**.

Naked-Eye Detection. A sensor, having a prominent color-changing property in the visual range upon interaction with analytes, is a potential candidate for the practical application, and this particular property of a sensor makes the preliminary qualitative analysis easier. To render the synthesized dialkyne moiety as a sensing probe, using its ground state complexation property, its visual detectability was qualitatively tested by naked eye. For that, each aforementioned metal ion (10^{-4} M) was added to a 10^{-4} M ligand solution, and it showed color changes from yellow to pale bluish green for Hg^{2+} and to light blue for Cu^{2+} and Fe^{3+} ions, respectively (Figure 6a), supporting the results obtained from the previous experiments. Thus, naked-eye detection makes the chemosensor molecule more susceptible to be applied practically. In fact, the quenching of fluorescence is also perceptible in the naked eye when the respective solutions of **5**, [**5**+ Hg^{2+}] (Figure 6), [**5**+ Cu^{2+}] and [**5**+ Fe^{3+}] (Figure S14) are irradiated under a 365 nm UV lamp in the dark. The irradiated pictures of **5** and [**5**+ Hg^{2+}] are given in Figure 6b to understand the quenching of fluorescence easily.

pH, Time, and Temperature Effects. Phenolphthalein is well-known to be pH sensitive,⁵⁴ and therefore, it has widely been used as an indicator in acid–base titration. Thus, our designed probe, containing phenolphthalein, is expected to show pH sensitivity. Although structural modification in the phenolphthalein unit was carried out by functionalizing the phenolic –OH groups, but still there is the lactone moiety that has pH sensitivity.^{55,56} Hence, the effects of pH on the fluorescence response of compound **5** and [**5**+ Hg^{2+}] complex are very important to be investigated to assess the overall applicability of the probe. A wide range of pH solutions from 2 to 12 in acetonitrile were prepared taking **5** (6.62×10^{-6} M) and [**5**+ Hg^{2+}] (6.62×10^{-6} M), and their corresponding fluorescence spectra were recorded immediately. The spectra show that fluorescence intensities and characteristics of the free ligand as well as the complexed moiety remain intact in the pH range of 6–7 but change erratically on moving left or right in the pH scale. This experiment evidently demonstrated that both compound **5** and [**5**+ Hg^{2+}] complex are stable in the biological pH range of 6–7 (Figure 7).

Thermal stability is another primary condition to be fulfilled for a molecule to be employed as a potential sensing probe. Our developed probe has a high degree of stability at room

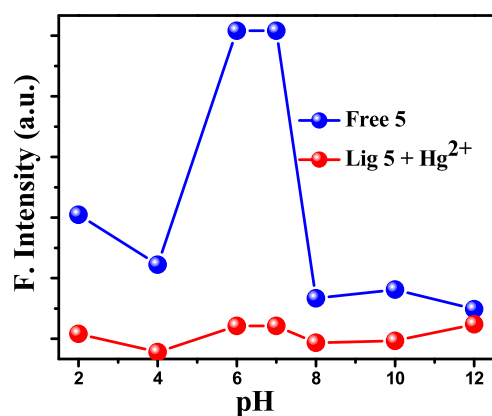


Figure 7. Fluorescence response of compound **5** (6.62×10^{-6} M) as a function of pH (pH 2–12) in the absence and presence of Hg^{2+} (2 equiv) (6.62×10^{-6} M) metal ion in CH_3CN at room temperature.

temperature, and it remains in the unperturbed form for months. To explore the stability over a range of temperatures, we have recorded fluorescence spectra of both receptor **5** and its Hg^{2+} complex, [**5**+ Hg^{2+}] in different temperatures (25–78 °C range) in acetonitrile solvent (Figure 8). The investigated results showed that the fluorescence intensity did not differ significantly with increasing temperature for both the free **5** (6.62×10^{-6} M) and [**5**+ Hg^{2+}] (6.62×10^{-6} M) system in acetonitrile. The unfluctuation in fluorescence intensities clearly indicated that the probe as well as the complexed entity are stable to temperature variation within the mentioned range. Since acetonitrile is used as the analytical solvent, fluorescence responses at temperatures above 78 °C could not be recorded.

A fast response time is a promoting factor for a sensor to be used in real time. Therefore, the response time of compound **5** toward Hg^{2+} ion (2 equiv) (6.62×10^{-6} M) in CH_3CN solution was investigated by recording the changes of the fluorescence intensity of the complexed species with time at room temperature. As depicted in Figure 9, Hg^{2+} ion interacted with compound **5** within 1 min of its addition to the ligand solution. This can be observed from the sudden minimization of fluorescence intensity of the complexed species within the first 1 min. However, the fluorescence intensity remains almost unaltered upon rerecording the spectra after certain time intervals up to 10 min. From this study, we can conclude that the present probe has the response time of <1 min, and this information will certainly allow this molecule to be used as a potential sensor probe.

Competitive Studies. After careful assessment about the nature of interaction of **5** with the three selected metal ions and the characteristics of the complexed species, we were curious to know about the extent of restoration of those individual interactions in the presence of each other metal ions (Hg^{2+} , Cu^{2+} , and Fe^{3+}). Therefore, a competitive experiment was carried out by electrochemical analysis. At first, 2 equiv of Cu^{2+} / Fe^{3+} ion was added into the CH_3CN solution of **5**, and it promoted the oxidation of ferrocene to ferrocenium ion in probe **5**, with no shift in potential in CV. Further, addition of 2 equiv of Hg^{2+} to this solution led to a shift in voltammetric wave toward anodic potential. This experiment indicated that Hg^{2+} ion is able to bind with the probe even after the oxidation of Fe(II) to Fe(III) of ferrocene unit of the probe (Figure 10a,b). Interestingly, the same result was observed even in the presence of excess amount of Cu^{2+} / Fe^{3+} ions. This experimental result demonstrated that the binding interaction of Hg^{2+} ion remained unchanged in the presence of other responding cations even in excess. Moreover, we have also performed the experiment in the reverse way, that is, addition of 2 equiv of Hg^{2+} followed by the addition of 2 equiv of Cu^{2+} / Fe^{3+} (Figure 10c,d). The results showed that even after binding to Hg^{2+} , oxidation of the Fe(II) of ferrocene unit occurs in the presence of Cu^{2+} / Fe^{3+} ion. Therefore, from this competitive experiment, we can conclude that the course of oxidation and binding are mutually exclusive, that is, they are independent of each other and do not interfere in each other's mechanism (Figure 11).

Real Sample Analysis. In order to investigate the practical utility, we have exposed our synthesized probe **5** toward the quantitative detection of Hg^{2+} ion in real water samples, collected from Jadavpur University campus. The water samples were filtered on a Whatman 41 filter paper, and their pH values were maintained around 6.5–7. Known concentrations of Hg^{2+} ion were added to the water samples separately, and cyclic voltammograms were recorded after addition of each aliquot of

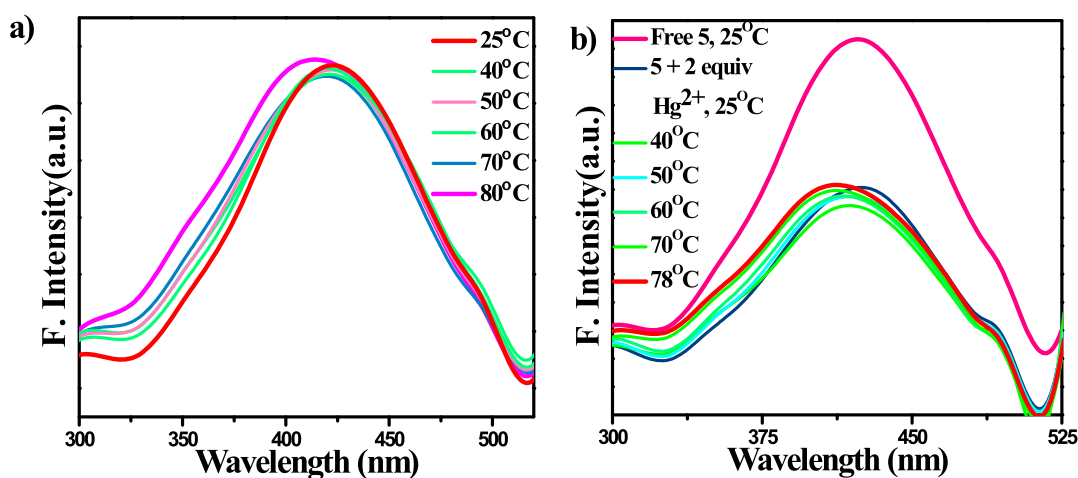


Figure 8. Temperature dependence of fluorescence intensity of (a) **5** (6.62×10^{-6} M) and (b) $[5+\text{Hg}^{2+}]$ (2 equiv) (6.62×10^{-6} M) in CH_3CN solution.

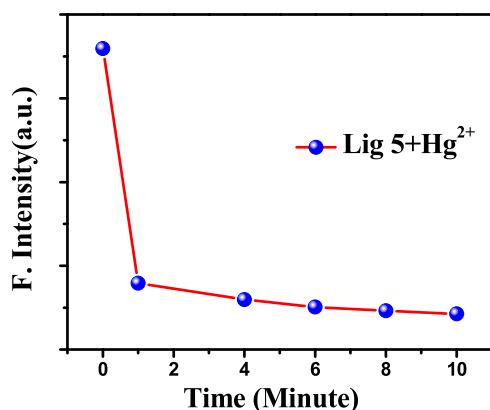


Figure 9. Time-dependent fluorescence intensity changes of compound **5** (6.62×10^{-6} M) upon addition of 2 equiv of Hg^{2+} (6.62×10^{-6} M) in CH_3CN solvent at room temperature.

aqueous solution of Hg^{2+} ion to the ligand solution in CH_3CN (6.25×10^{-5} M). With each addition, shifts in potential were obtained for both water samples. The corresponding recovered Hg^{2+} ion concentrations were calculated from the equations $y = (3642x - 0.014)$ and $y = (2908x - 0.004)$, with correlation coefficients $R^2 = 0.988$ and $R^2 = 0.992$ for pond water and tap water samples, respectively (Figure S15). The experimental concentration and percentage recovery values are shown in Table 2.

DFT Studies. In order to get the detailed information about the electronic structure and to understand the bonding scenario of the receptor toward Hg^{2+} , we have performed theoretical studies at the DFT level of theory. At first, few possible starting geometries are taken to optimize the geometry to obtain the global minima and geometry optimization of **5** and $[5 \cdot 2\text{Hg}^{2+}]$ was done by DFT calculations at B3LYP-D3/def2-SVP level of theory.⁵⁷ Their corresponding molecular orbital pictures are shown in Supporting Information (Figures S16 and S17). The optimized structure of the receptor **5** showed a linear structure of middle 1,3-dialkyne unit, and the two phenolphthalein-ferrocene moieties are oriented in *trans* fashion with respect to each other (Figure 12). Bond lengths are given respectively as C1–C2:1.496 Å; C2–C3:1.250 Å; C3–C4:1.407 Å; C4–C5:1.25 Å; C5–C6:1.496 Å. Analysis of bond lengths indicated a relatively shorter C3–C4 single bond which connects the two

alkyne units, and this observation is in agreement with literature reports.^{41,42} Further, it is confirmed by natural bond orbital (NBO) analysis at the same level of theory. Wiberg bond indices of the C1–C2, C2–C3, C3–C4, C4–C5, and C5–C6 bonds are 1.071, 2.610, 1.214, 2.610, and 1.070, respectively. The detailed bond lengths and Wiberg bond indices are depicted in Table S1.

Now in order to understand the exact binding site of Hg^{2+} with receptor **5**, we have performed theoretical calculation with different model systems. We have tried to optimize all the possible structures of metal complexes with different binding sites and calculated their corresponding binding energies. Among all the possible geometries, the structure in which two Hg^{2+} ions bind with conjugated 1,3-diyne unit is the energy-minimized structure with most stable conformation (Figure 13). This result supports our experimental findings where the ligand to metal binding ratio was found to be 1:2. The binding energy of this optimized geometry is significantly high (13.64 kcal/mol) as compared to the other optimized structures. Another geometry optimized structure involving O atom of $-\text{OCH}_2-$ unit adjacent to alkyne (Figure S18) also exhibits the similar kind of binding energy (14.43 kcal/mol). However, from the experimental results obtained from ^1H NMR and ^{13}C NMR titrations, the possibility of this optimized model can be eliminated as no shift of $-\text{OCH}_2-$ is observed in ^1H NMR as well as ^{13}C NMR titration of receptor **5** after addition of Hg^{2+} ion. Furthermore, natural bond analysis (NBO) at B3LYP-D3/def2-SVP level is performed to get insight of the bonding pattern of the $[5 \cdot 2\text{Hg}^{2+}]$. Bond lengths (and WBI) are given as C1–C2:1.457 Å (1.071); C2–C3:1.220 Å (2.589); C3–C4:1.370 Å (1.215); C4–C5:1.220 Å (2.589); C5–C6:1.457 Å (1.072). From the energy minimized structure of the **5** and $[5 \cdot 2\text{Hg}^{2+}]$, we have observed that there is a change in alkyne bond lengths (1.25 Å to 1.22 Å) and middle C3–C4 bond length (1.40 Å to 1.37 Å) upon coordination of mercury to the receptor, indicating a weak interaction of the receptor with Hg^{2+} ion. To confirm it further we have done NBO calculation, which depicts a small change in Weiberg Bond Index from 2.610 to 2.589. This small change in WBI indicates the weak interaction of π -orbital of alkyne with the mercury ion.

In the optimized structure, the bond distance between Hg and carbon atoms are in the range of 3.2–3.6 Å which corroborates the value reported in the literature.⁵⁸ Therefore, from ^1H , ^{13}C

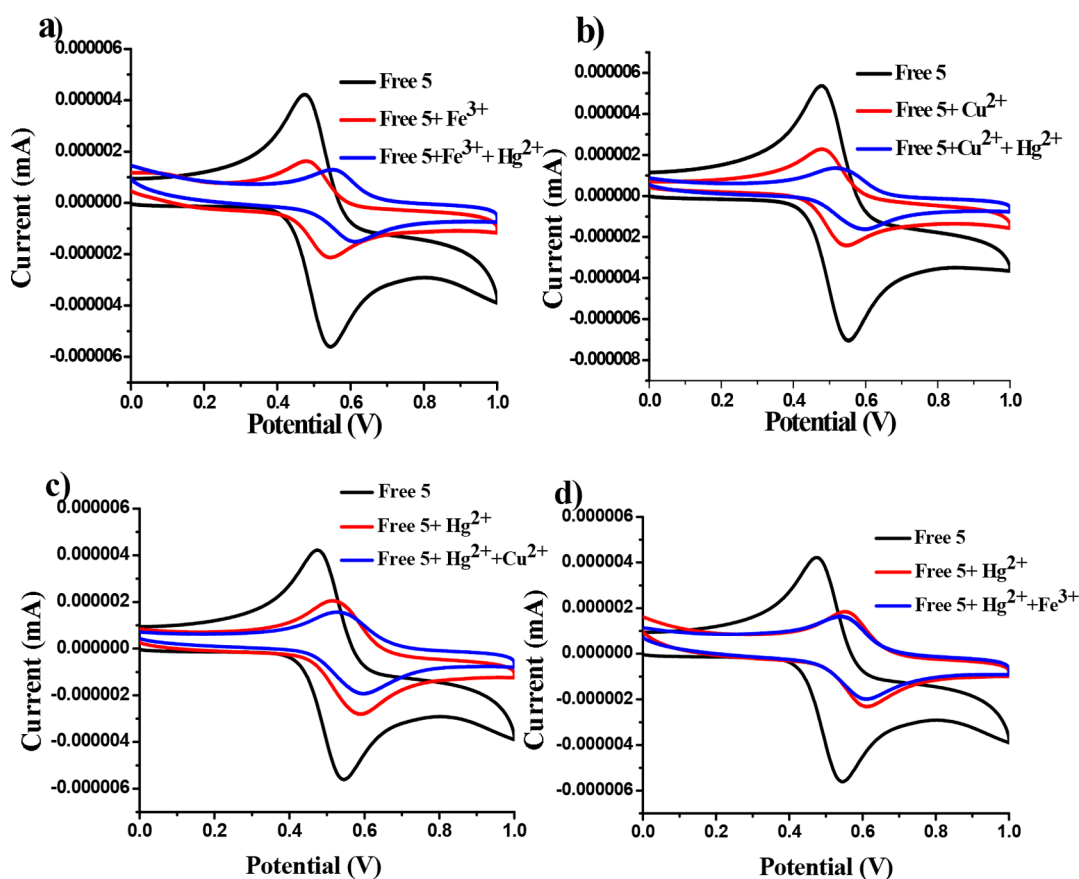


Figure 10. Competitive experiments with (a) and (d) Fe^{3+} and Hg^{2+} ; (b) and (c) Cu^{2+} and Hg^{2+} in CH_3CN solvent at room temperature.

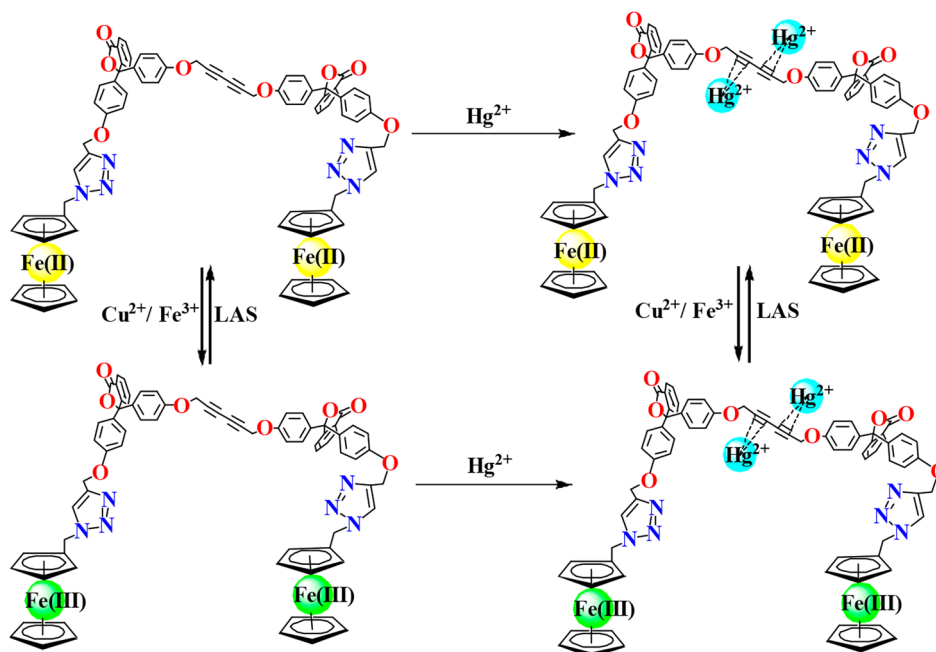


Figure 11. Schematic representation of binding mode with Hg^{2+} ion and competitive nature of interaction with all three metal ions.

NMR titrations and the combined DFT analysis, it is confirmed that 2 Hg^{2+} ions bind with the 1,3-dialkyne unit of the receptor and provided the more stable conformation.

Further, to rationalize the detailed information about the UV-vis spectra, time-dependent DFT (TD-DFT) calculations

at the B3LYP-D3/def2-SVP/CPCM (acetonitrile) level were performed. TD-DFT vertical excited state calculations of the receptor 5 predicts a HOMO-28 (phenolphthalein π type) to LUMO+1 (phenolphthalein π^* type) transition with the band centered at 224 nm (oscillator strength $f = 0.18$) (Table S2),

Table 2. Determination of Recovered Concentrations of Hg²⁺ Ion in Pond Water and Tap Water Samples

samples	added metal concn (M)	recovered metal concn (M)	% of recovery	% error
pond water	1.69×10^{-5}	1.68×10^{-5}	99.40	0.5
tap water	2.35×10^{-5}	2.31×10^{-5}	98.29	1.7

which is in close agreement with the experimental results. Similarly, TD-DFT calculations at the B3LYP-D3/def2-SVP/CPCM (acetonitrile) level on [5·2Hg²⁺] predict a strong HOMO–29 (phenolphthalein π type) to LUMO+4 (phenolphthalein π^* type) (Table S3) transition with the band centered at 225 nm (oscillator strength $f = 0.14$), and this is also in close agreement with the experimental UV–vis results. The calculated gaps between the orbitals involved in major transitions for both 5 and [5·2Hg²⁺] complex are in the same range (5.91 and 5.92 eV, respectively), which demonstrates no significant shifts in UV–vis absorption bands, and this is clearly concurrent with the experimental findings.

Furthermore, to shed more light on fluorescence quenching mechanism, TD-DFT calculations were done at the same level of theory. TD-DFT calculations revealed that the mercury-centered empty orbital (LUMO) lies between the fluorophore (phenolphthalein) transition orbitals (Figure 14). As a result, the electron in the excited state of the phenolphthalein-centered orbital (LUMO+4) was transferred to the energetically favorable mercury-centered empty orbital (LUMO) instead of highly buried HOMO–29 state. Therefore, this type of orientation of orbitals might be providing an additional pathway for fluorescence quenching of receptor in the presence of Hg²⁺ ion.

CONCLUSIONS

Herein, we have designed and synthesized a C₂-symmetric internally conjugated 1,3-dialkyne system via microwave-assisted synthetic procedure in neat condition for the first time. The microwave-assisted synthesis of the probe in solution phase as well as in neat condition has paved the way for further modulation of greener ways in synthetic methodology. To the best of our knowledge, this is the first report of a conjugated 1,3-

diyne system, which has been exploited as a Hg²⁺ ion sensor. The synthesized molecule, containing ferrocene as redox unit and phenolphthalein as a fluorophore, was found to be highly selective toward the detection of Hg²⁺ ion whereas Fe³⁺ and Cu²⁺ merely promote the oxidation of ferrocene unit. In addition, our designed probe was successfully explored toward the detection of Hg²⁺ ion in real water samples. Two Hg²⁺ ions bind with two-alkyne motifs by “soft–soft” interaction and this mode of binding was supported by NMR titration and DFT calculations along with optical and electrochemical experiments. We believe that we have demonstrated a new strategy using conjugated 1,3-diyne unit for direct detection of Hg²⁺ using the concept of HSAB principle.

EXPERIMENTAL SECTION

Materials and Reagents. Among the metal ions used, Na⁺, K⁺, Fe²⁺, Fe³⁺, Cu²⁺, and Hg²⁺ were purchased from Sigma-Aldrich, and Ag⁺, Ca²⁺, Mg²⁺, Mn²⁺, Zn²⁺, Pb²⁺, Co²⁺, Cr³⁺, and Al³⁺ were purchased from Alfa Aesar, as their respective perchlorate salts, and used directly without further purification. Cu⁺ was purchased from Sigma-Aldrich as [(CH₃CN)₄Cu]PF₆. NaH was purchased from Sigma-Aldrich, and Glacial AcOH was obtained from Merck. DMF and acetonitrile (HPLC) were purchased from Thermo Fisher Scientific and freshly distilled prior to use. The remaining chemicals were purchased from a local brand. Mono(azidomethyl)ferrocene was prepared according to literature reported procedure.⁵⁹ Chromatography was carried out using 60–120 mesh silica gel in a column of 2.5 cm diameter. All the necessary solvents were dried by conventional methods and distilled under N₂ atmosphere. The cyclic voltammetry (CV) was performed with a conventional three-electrode configuration consisting of glassy carbon as working electrode, platinum as an auxiliary electrode, and Ag/Ag⁺ as a reference electrode. The experiment was carried out with a 10^{−4} M solution of sample in CH₃CN containing 0.1 M (TBAP) [(*n*-C₄H₉)₄NClO₄] as supporting electrolyte. The working electrode was cleaned after each run. The cyclic voltammograms were recorded at a scan rate 0.05 V s^{−1}, and readings were taken considering ferrocene/ferrocenium couple as the standard. The UV–vis spectra were carried out in CH₃CN solutions at $c = 10^{-6}$ M and the fluorescence spectra were carried out at $c = 10^{-6}$ M, as stated in the corresponding figure captions.

Preparation of IR Samples. The compound 5 and 1 and 2 equiv of Hg(ClO₄)₂ were weighed separately and dissolved in acetonitrile and then mixed together correspondingly to form 5+1 equiv of Hg²⁺ and 5+2 equiv of Hg²⁺. The acetonitrile was then dried in a rotary

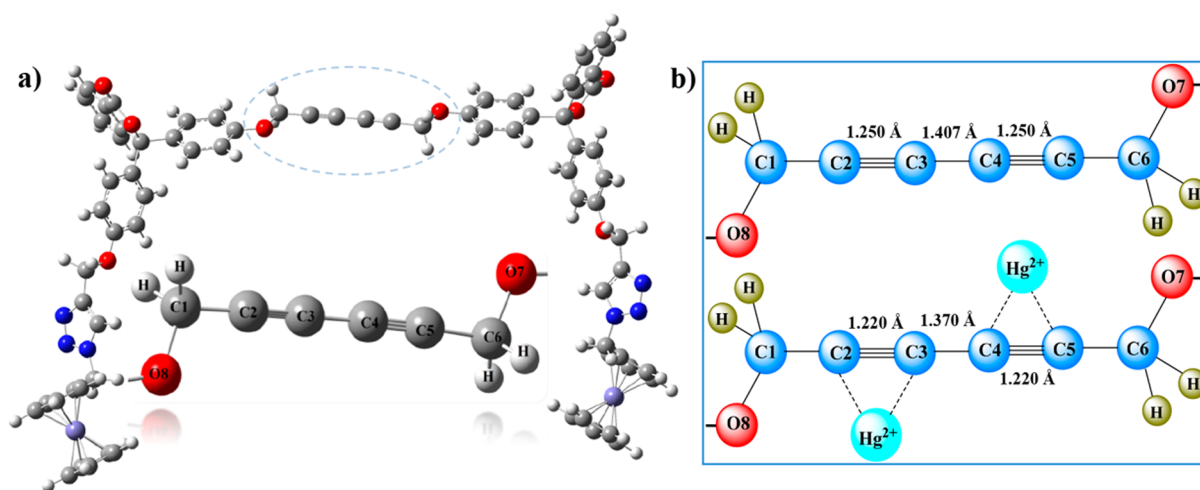


Figure 12. (a) Optimized structure of the receptor 5. Zoomed structure of middle unit of receptor 5 to understand the bonding (inset). (b) Chemdraw structure of the conjugated binding unit before and after binding with Hg²⁺ along with the C–C bond lengths.

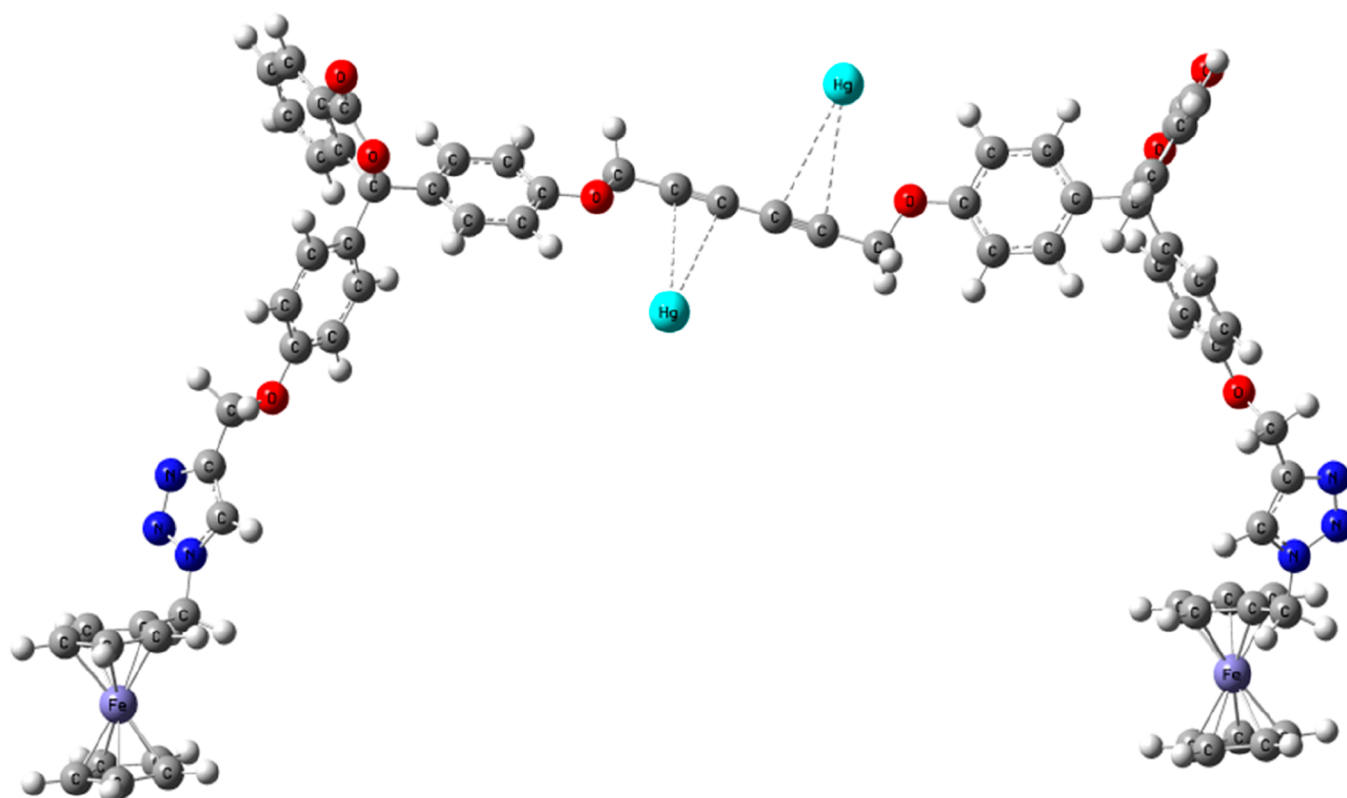


Figure 13. Optimized structure of the complex $[5 \cdot 2\text{Hg}^{2+}]$.

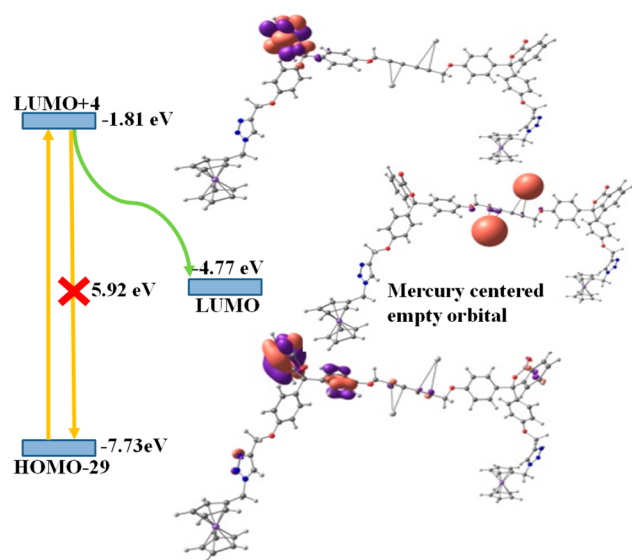


Figure 14. Schematic representation of fluorescence quenching due to Hg^{2+} ion binding to the receptor.

evaporator and stored under vacuum for some time. Thus, we obtained two sets of complexed species in the solid form. The IR spectra of the free ligand with these two sets of samples were recorded in solid form.

Preparation of Samples for Elemental Analysis of the Complex Species. For the elemental analysis of the $[5 \cdot 2\text{Hg}^{2+}]$ complex, pure 5 was taken in a minimum amount of dichloromethane; then 2 molar equiv of $\text{Hg}(\text{ClO}_4)_2$ was dissolved in CH_3CN , and the two solutions were mixed up gradually. The solvent mixture was evaporated in a rotary evaporator and then stored under vacuum for some time. The resulting green solid compound was washed several times with water to remove free perchlorate anion, followed by washed with dichloromethane and kept under high vacuum for 5 h. This sample was

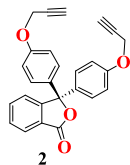
used for analysis. Anal. Calcd for $\text{C}_{74}\text{H}_{56}\text{Fe}_2\text{N}_6\text{O}_8\text{Hg}_2$: C, 53.10; H, 3.34; N, 5.02. Found: C, 54.04; H, 4.01; N, 5.54.

Instrumentation. ^1H and ^{13}C NMR spectra were obtained with BRUKER 400 and 300 MHz FT-NMR spectrometers, respectively. For compound 2, both ^1H and ^{13}C NMR spectra have been taken in BRUKER 300 MHz FT-NMR spectrometer. The chemical shifts are reported in ppm, using tetramethylsilane as an internal standard, and were referenced to the residual solvent as follows: $\text{CDCl}_3 = 7.26$ (^1H), 76.16 (^{13}C) ppm, $\text{DMSO} = 2.51$ (^1H), 39.50 (^{13}C) at room temperature. For ^1H NMR, coupling constants J are given in Hz, and the resonance multiplicity is described as s (singlet), d (doublet), t (triplet), m (multiplet). IR spectral studies were done with a PerkinElmer LX-1 FTIR spectrophotometer. The absorption spectra were recorded with a SHIMADZU-2450 UV-vis spectrophotometer at room temperature. Fluorescence was recorded with SHIMADZU RF-5301pc spectrophotometer. CH Instruments Electrochemical Analyzer was used to perform the cyclic voltammetry (CV) and differential pulse voltammetry (DPV) studies. HRMS were taken using Quadruple-TOF (Q-TOF) micro MS system using electrospray ionization (ESI) technique. CHN analysis was performed on a Vario EL elemental CHNS analyzer. Microwave optimization has been done in CEM microwave.

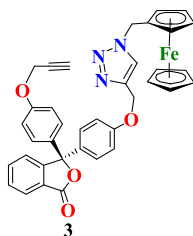
Caution! Metal perchlorate salts are potentially explosive in certain conditions. All due precautions should be taken while handling perchlorate salts!

Synthesis of Compounds 2, 3, and 5. Synthesis of Compound 2. Phenolphthalein (500 mg, 1.57 mmol) was taken in a clean round-bottomed flask and dissolved in 10 mL of DMSO solvent. K_2CO_3 (867 mg, 6.28 mmol) was added to the solution and kept to stir for 30 min after which propargyl bromide (0.5 mL, 6.28 mmol) was added and stirring was continued overnight. The reaction mixture was extracted with EtOAc and dried over Na_2SO_4 , and the solvent was dried under vacuum. Column chromatography in 20% EtOAc in hexane gave pure compound 2 (3,3-bis(4-(prop-2-yn-1-yloxy)phenyl)isobenzofuran-1(3H)-one) (499 mg, 80% yield). ^1H NMR (CDCl_3 , 300 MHz) $\delta = 7.91$ (d, 1H, H_{aromatic} , $J = 6$ Hz), 7.70–7.67 (m, 1H, H_{aromatic}), 7.58–7.52 (m, 2H, H_{aromatic}), 7.30–7.25 (m, 4H, H_{aromatic}), 6.96–6.91 (m, 4H,

H_{aromatic}), 4.68 (d, 4H, $J = 2.4$ Hz, OCH_2), 2.53 (t, 2H, $J = 2.4$ Hz, H_{alkyne}); ^{13}C NMR (CDCl_3 , 75 MHz) $\delta = 169.78, 157.63, 152.37, 134.25, 133.92, 129.34, 128.57, 125.96, 125.49, 124.07, 114.72, 91.42, 78.32, 75.95, 55.81$; HRMS m/z calcd for $\text{C}_{26}\text{H}_{18}\text{O}_4$ [$\text{M} + \text{Na}$] $^+$, 417.1102; found, 417.0885.



Synthesis of Compound 3. 3,3-Bis(4-(prop-2-yn-1-yloxy)phenyl)-indobenzofuran-1(3H)-one (**2**) (1g, 2.53 mmol) and 0.9 equiv of mono(azidomethyl)ferrocene (554.48 mg, 2.3 mmol) were taken in a 100 mL round-bottom flask and dissolved in $^t\text{BuOH}$ (26 mL) solvent. $\text{CuSO}_4 \cdot 5\text{H}_2\text{O}$ and sodium-L-ascorbate were dissolved in a total of 13 mL of H_2O and added to the reaction mixture one by one at room temperature. After 1 h, a greenish suspension was formed, which was allowed to stir overnight at room temperature. Reaction mixture was diluted with ethyl acetate and washed with distilled water. The organic phase was separated and dried over sodium sulfate, and the solvent was removed under reduced pressure. Then the crude product was purified by silica gel column chromatography. Elution with 40% EtOAc/hexane gave yellow colored solid compound **3** (550 mg, 0.86 mmol, yield 35%) along with some amount of compound **4** (0.5 mmol, yield 20%) as side product. **3**: ^1H NMR (CDCl_3 , 400 MHz) $\delta = 7.93$ (d, 1H, $J = 8$ Hz, H_{aromatic}), 7.69 (t, 1H, $J = 8$ Hz, H_{aromatic}), 7.57 (s, 1H, H_{aromatic}), 7.55 (s, 1H, H_{triazole}), 7.51 (d, 1H, $J = 8$ Hz, H_{aromatic}), 7.22–7.28 (m, 4H, H_{aromatic}), 6.92 (d, 4H, $J = 8$ Hz, H_{aromatic}), 5.30 (s, 2H, OCH_2), 5.15 (s, 2H, NCH_2), 4.68 (s, 2H, OCH_2), 4.28 (s, 2H, H_{Fc}), 4.22 (s, 2H, H_{Fc}), 4.17 (s, 5H, H_{Fc}), 2.53 (s, 1H, H_{alkyne}); ^{13}C NMR (CDCl_3 , 75 MHz) $\delta = 169.77, 158.32, 157.61, 152.42, 143.67, 134.12, 133.97, 133.52, 129.25, 128.65, 128.49, 125.96, 125.55, 124.02, 122.15, 114.70, 114.64, 91.45, 80.72, 78.27, 75.80, 69.09, 68.92, 62.061, 55.83, 50.16, 30.91$; HRMS m/z calcd for $\text{C}_{37}\text{H}_{29}\text{FeN}_3\text{O}_4$ [M] $^+$ 635.1507; found 635.1900; Anal. Calcd for $\text{C}_{37}\text{H}_{29}\text{FeN}_3\text{O}_4$: C, 69.93; H, 4.60; N, 6.61. Found: C, 69.63; H, 4.48; N, 6.42.



Synthesis of Compound 5. The coupling reaction of compound **3** had been performed by two ways: one by slight modification of the already established procedure³⁶ and another by taking the assistance of a single focus microwave in a closed reaction system.

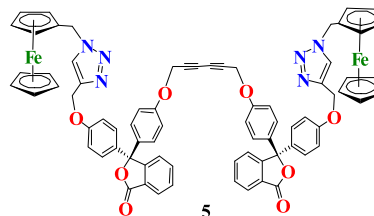
By the conventional method: Compound **3** (206 mg, 0.324 mmol) and 15 equiv of $\text{Cu}(\text{OAc})_2 \cdot \text{H}_2\text{O}$ (971.25 mg, 4.86 mmol) were added in a 100 mL round-bottom flask and dissolved in pyridine solvent (15 mL). The reaction mixture was stirred at room temperature for 2 h and then at 60 °C for 2 h. The blue reaction mixture was cooled to room temperature, and the stirring was continued for further 48 h. Cold water was added after which brown precipitate appeared, and the reaction mixture was stirred for another 10 min. Filtration of the brown precipitate under suction and successive washings with water and finally with ethanol gave us dry pyridine free product, which on further purification by silica gel column chromatography (60% EtOAc/Hex) gave a pale yellow colored solid compound **5** (61 mg, yield 29.67%).

Microwave-assisted reaction: This was done in closed reaction system whereby compound **3** (100 mg, 0.16 mmol) was taken into the closed system vessel containing a rice magnet, dissolved in pyridine solvent (5 mL), and then the catalyst $\text{Cu}(\text{OAc})_2 \cdot \text{H}_2\text{O}$ (3 equiv, 100 mg, 0.5 mmol) was added. When the catalyst got dissolved totally, the vessel

was put to microwave radiation in the reactor under 50 W power maintaining a constant 60 °C for 30 min. After reaction vessel was cooled, it was taken out, and the color of the reaction mixture was observed to change from green (before the reaction) to yellowish green (after the reaction). The reaction mixture was poured into a vessel containing cold water (7 mL) and was left for sometime, after which brown precipitate can be observed. It was filtered and washed successively with water (5×10 mL) and finally with ethanol (2 mL). The precipitate was redissolved in DCM and further purification was done by silica gel column chromatography after which pure **5** was obtained (91 mg, 0.072 mmol, yield 90%).

For the neat reaction, **3** (50 mg, 0.078 mmol) was grinded well with 3.7 equiv of $\text{Cu}(\text{OAc})_2 \cdot \text{H}_2\text{O}$ (58 mg, 0.29 mmol) until a homogeneous powder was formed. Then it was poured into the glass tube for a closed vessel reaction system along with 3 equiv of pyridine as base (19 μL , 0.234 mmol). It was mixed properly and then subjected to microwave irradiation at 50 W power and 60 °C for 30 min. Then it was cooled down and washed successively with water to remove any traces of pyridine. Finally, work up in EtOAc and removing the solvent under vacuum after drying on sodium sulfate gave compound **5** with 80% conversion of compound **3**.

^1H NMR (CDCl_3 , 400 MHz) $\delta = 7.91$ (d, 1H, $J = 8$ Hz, H_{aromatic}), 7.67 (t, 1H, $J = 8$ Hz, H_{aromatic}), 7.53 (t, 1H, $J = 8$ Hz, H_{aromatic}), 7.49 (s, 1H, H_{triazole}), 7.48 (s, 1H, H_{aromatic}), 7.21 (t, 4H, $J = 8$ Hz, H_{aromatic}), 6.91–6.85 (m, 4H, H_{aromatic}), 5.26 (s, 2H, OCH_2), 5.13 (s, 2H, OCH_2), 1.63 (s, 2H, NCH_2), 4.26 (s, 2H, H_{Fc}), 4.21 (s, 2H, H_{Fc}), 4.16 (s, 5H, H_{Fc}); ^{13}C NMR (d_6 -DMSO, 75 MHz) $\delta = 169.41, 158.26, 157.22, 152.19, 142.77, 135.38, 134.07, 133.22, 130.20, 128.45, 128.42, 125.87, 124.70, 124.55, 118.49, 115.08, 91.16, 82.63, 76.19, 70.35, 68.95, 68.91, 68.71, 61.26, 56.01, 49.31$; HRMS (ESI) m/z calcd for $\text{C}_{74}\text{H}_{56}\text{Fe}_2\text{N}_6\text{O}_8$ [$\text{M} + \text{H}$] $^+$, 1269.2937; found, 1269.2935; Anal. Calcd for $\text{C}_{74}\text{H}_{56}\text{Fe}_2\text{N}_6\text{O}_8$: C, 70.03; H, 4.45; N, 6.63. Found: C, 69.43; H, 4.38; N, 6.39.



Computational Studies. All computational calculations presented in this paper were performed by density functional theory (DFT) method using the Gaussian 16⁶⁰ program package. Full geometry optimizations were carried out using the B3LYP (Becke, three parameter, Lee–Yang–Parr)-D3 level of theory.⁶¹ The def2-SVP⁵⁷ basis set was employed for all the atoms with the conductor-like polarizable continuum model⁶² (CPCM) using acetonitrile as a solvent. The vibrational frequency calculations were performed to ensure that the optimized geometries represent the local minima and that there are only positive eigenvalues. Natural bond orbital (NBO) analysis⁶³ and Wiberg bond indices (WBI)⁶⁴ were performed at the same level^{57,61} using the NBO Version 3.1 program implemented in the Gaussian package. Orbital diagrams are rendered in the Chemcraft visualization software with an isosurface value 0.04.⁶⁵

ASSOCIATED CONTENT

Supporting Information

The Supporting Information is available free of charge at <https://pubs.acs.org/doi/10.1021/acs.inorgchem.0c01236>.

^1H , ^{13}C and HRMS data of compound **2**, **3** and **5**. UV–vis spectra, fluorescence spectra and cyclic voltammetric plot with Fe^{3+} , Cu^{2+} as also with different metal ions, quantitative binding data and LOD by $3\sigma/S$ for **5** with Hg^{2+} , DFT optimized alternate structure of binding of Hg^{2+} with **5**, bond distance table and excited state transitions with oscillator strength tables for both **5** and

[5+2Hg²⁺]. Cartesian coordinates of ligand **5**, and [5-2Hg²⁺] with the two alternate binding modes. IR titration plot of **5** with Hg²⁺. Regression plots for real samples analysis (PDF)

AUTHOR INFORMATION

Corresponding Author

Arunabha Thakur – Department of Chemistry, Jadavpur University, Kolkata 700032, India; orcid.org/0000-0003-4577-3683; Phone: 0332-4572779; Email: arunabha.thakur@jadavpuruniversity.in, babuiit07@gmail.com

Authors

Adwitiya Pal – Department of Chemistry, Jadavpur University, Kolkata 700032, India

Krishna Mohan Das – Department of Chemistry, Jadavpur University, Kolkata 700032, India

Bappaditya Goswami – Department of Chemical Sciences, Indian Institute of Science Education and Research Kolkata, Mohanpur 741246, India

Complete contact information is available at:
<https://pubs.acs.org/10.1021/acs.inorgchem.0c01236>

Notes

The authors declare no competing financial interest.

ACKNOWLEDGMENTS

RUSA 2.0 is gratefully acknowledged for financial support to carry out the research work. AP and KMD acknowledge CSIR and UGC for providing JRF fellowships respectively. BG is thankful to the IISER Kolkata for the fellowship.

REFERENCES

- (1) Shi, W.; Lei, A. 1,3-Diyne chemistry: synthesis and derivations. *Tetrahedron Lett.* **2014**, *55*, 2763–2772.
- (2) Liu, J.; Lam, W. Y. J.; Tang, B. Z. Acetylenic polymers: syntheses, structures and functions. *Chem. Rev.* **2009**, *109*, 5799–5867.
- (3) Michl, J.; Sykes, E. C. H. Molecular rotors and motors: recent advances and future challenges. *ACS Nano* **2009**, *3*, 1042–1048.
- (4) Wu, S. T.; Meng, H. H. B.; Dalton, L. R. Diphenyl-diacetylene liquid crystals for electro-optic application. *J. Appl. Phys.* **1991**, *70*, 3013–3017.
- (5) Wu, S. T.; Margerum, J. D.; Meng, H. B.; Dalton, L. R.; Hsu, C. S.; Lung, S. H. Room-temperature diphenyl-diacetylene liquid crystals. *Appl. Phys. Lett.* **1992**, *61*, 630–632.
- (6) Wu, S. T.; Neubert, M. E.; Keast, S. S.; Abdallah, D. G.; Lee, S. N.; Walsh, M. E.; Dorschner, T. A. Wide nematic range alkenyldiphenyldiacetylene liquid crystals. *Appl. Phys. Lett.* **2000**, *77*, 957–959.
- (7) Beristain, M. F.; Ogawa, T.; Gomez-Sosa, G.; Munoz, E.; Maekawa, Y.; Halim, F.; Smith, F.; Walser, A.; Dorsinville, R. Polymerization of diphenylbutadiene by gamma rays irradiation in the molten state. *Mol. Cryst. Liq. Cryst.* **2010**, *521*, 237–245.
- (8) Sari, O.; Roy, V.; Balzarini, J.; Snoeck, R.; Andrei, G.; Agrofoglio, L. A. Synthesis and antiviral evaluation of C5 substituted-(1, 3-diyne)-2'-deoxyuridines. *Eur. J. Med. Chem.* **2012**, *53*, 220–228.
- (9) Kivala, M.; Diederich, F. Conjugation and optoelectronic properties of acetylenic scaffolds and charge-transfer chromophores. *Pure Appl. Chem.* **2008**, *80*, 411–427.
- (10) McConnell, A. J.; Beer, P. D. Kinetic studies exploring the role of anion temptation in the slippage formation of rotaxane-like structures. *Chem. - Eur. J.* **2011**, *17*, 2724–2733.
- (11) Sugino, H.; Kawai, H.; Umehara, T.; Fujiwara, K.; Suzuki, T. Effects of axle-core, macrocycle, and side-station structures on the threading and hydrolysis processes of imine-bridged rotaxanes. *Chem. - Eur. J.* **2012**, *18*, 13722–13732.
- (12) Langton, M. J.; Matchak, J. D.; Thompson, A. L.; Anderson, H. L. Template-directed synthesis of π -conjugated porphyrin[2]rotaxanes and a [4]catenene based on a six-porphyrin nano ring. *Chem. Sci.* **2011**, *2*, 1897–1901.
- (13) Shi Shun, A. L. K.; Tykwinski, R. R. Synthesis of naturally occurring polyyenes. *Angew. Chem., Int. Ed.* **2006**, *45*, 1034–1057.
- (14) Hu, R.; Tang, B. Z. In *Multi-Component and Sequential Reactions in Polymer Synthesis*; Theato, P., Ed.; Springer International Publishing: Switzerland, 2015; pp 17–42.
- (15) Vilhanova, B.; Vaclavik, J.; Artiglia, L.; Ranocchiaro, M.; Togni, A.; van Bokhoven, J. A. Subnanometer gold clusters on amino-functionalized silica: an efficient catalyst for the synthesis of 1, 3-diyne by oxidative alkyne coupling. *ACS Catal.* **2017**, *7*, 3414–3418.
- (16) Eglinton, G.; Galbraith, A. R. Macrocyclic acetylenic compounds. Part I. Cyclotetradeca 1, 3-diyne and related compounds. *J. Chem. Soc.* **1959**, 889–896.
- (17) Hay, A. S. Oxidative coupling of acetylenes. II. *J. Org. Chem.* **1962**, *27*, 3320–3321.
- (18) Pati, A. K.; Mohapatra, M.; Ghosh, P.; Gharpure, S. J.; Mishra, A. K. Deciphering the photophysical role of conjugated diyne in butadiynylfluorophores: synthesis, photophysical and theoretical study. *J. Phys. Chem. A* **2013**, *117*, 6548–6560.
- (19) Wang, D.; Li, J.; Li, N.; Gao, T.; Hou, S.; Chen, B. An efficient approach to homocoupling of terminal alkynes: solvent-free synthesis of 1,3-diyne using catalytic Cu(II) and base. *Green Chem.* **2010**, *12*, 45–48.
- (20) Atta, A. K.; Kim, S. B.; Heo, J.; Cho, D. G. Hg (II)-mediated intramolecular cyclization reaction in aqueous medium and its application as Hg (II) selective indicator. *Org. Lett.* **2013**, *15*, 1072–1075.
- (21) Dong, M.; Wang, Y. W.; Peng, Y. Highly selective ratiometric fluorescent sensing for Hg²⁺ and Au³⁺ respectively in aqueous media. *Org. Lett.* **2010**, *12*, 5310–5313.
- (22) Tian, M.; Liu, L.; Li, Y.; Hu, R.; Liu, T.; Liu, H.; Wang, S.; Li, Y. An unusual off-on fluorescence sensor for detecting mercury ions in aqueous media and living cell. *Chem. Commun.* **2014**, *50*, 2055–2057.
- (23) Kaur, M.; Choi, D. H. Dual channel receptor based on diketopyrrolopyrrole alkyne conjugated for detection of Hg²⁺/Cu²⁺ by naked eye and fluorescence. *Sens. Actuators, B* **2014**, *190*, 542–548.
- (24) Lee, D. N.; Kim, G. J.; Kim, H. J. A fluorescent coumarinyl alkyne probe for the selective detection of Hg (II) ion in water. *Tetrahedron Lett.* **2009**, *50*, 4766–4768.
- (25) Chattaraj, P. K.; Lee, H.; Parr, R. G. HSAB Principle. *J. Am. Chem. Soc.* **1991**, *113*, 1855–1856.
- (26) Harris, H. H.; Pickering, I. J.; George, G. N. The chemical form of mercury in fish. *Science* **2003**, *301*, 1203.
- (27) Onyido, I.; Norris, A. R.; Buncel, E. Biomolecule-mercury interactions: modalities of DNA base-mercury binding mechanisms. *Chem. Rev.* **2004**, *104*, 5911–5922.
- (28) Bernhoff, R. A. Mercury toxicity and treatment: A review of the literature. *J. Environ. Public Health* **2012**, *2012*, 460508.
- (29) Toyota, S.; Oki, T.; Inoue, M.; Wakamatsu, K.; Iwanaga, T. Cramping an alkyl group by rigid macrocyclic framework. *Chem. Lett.* **2015**, *44*, 978–980.
- (30) He, X.; Liu, H.; Li, Y.; Wang, S.; Li, Y.; Wang, N.; Xiao, J.; Xu, X.; Zhu, D. Gold nanoparticle-based fluorometric and colorimetric sensing of copper (II) ions. *Adv. Mater.* **2005**, *17*, 2811–2815.
- (31) Nolan, E. M.; Lippard, S. J. Tools and tactics for the optical detection of mercuric ion. *Chem. Rev.* **2008**, *108*, 3443–3480.
- (32) Aragay, G.; Pons, J.; Merkoci, A. Recent trends in macro, micro and nanomaterial-based tools and strategies for heavy-metal detection. *Chem. Rev.* **2011**, *111*, 3433–3458.
- (33) Jia, K.; Zhou, X.; Pan, L.; Yuan, L.; Wang, P.; Wu, C.; Huang, Y.; Liu, X. Plasmon enhanced fluorescence of a bisphthalonitrile-based dye via a dopamine mediated interfacial crosslinking reaction on a silver nanoparticles. *RSC Adv.* **2015**, *5*, 71652–71657.

- (34) Erdemir, S.; Malkondu, S.; Kocyigit, O. A reversible calix[4]arene armed phenolphthalein based fluorescent probe for the detection of Zn²⁺ and an application in living cells. *Luminescence* **2019**, *34*, 106–112.
- (35) Sun, R.; Wang, L.; Yu, H.; Abdin, Z.; Chen, Y.; Huang, J.; Tong, R. Molecular recognition and sensing based on ferrocene derivatives and ferrocene-based polymers. *Organometallics* **2014**, *33*, 4560–4573.
- (36) Behr, O. M.; Eglinton, G.; Galbraith, R. A.; Raphael, R. A. Macrocyclicacetylenic compounds. part II. 1, 2:7, 8-dibenxocyclododeca-1, 7-diene-3, 5, 9, 11-tetraene. *J. Chem. Soc.* **1960**, 3614–3625.
- (37) Sharifi, A.; Mirzaei, M.; Naimi-Jamal, M. R. Copper-catalyzed oxidative homo-coupling of terminal acetylenes on alumina assisted by microwave irradiation. *J. Chem. Res.* **2002**, *2002*, 628–630.
- (38) Liu, Z.; Liu, J.; Chen, T. Facile synthesis, characterization, and potential application of two kinds of polymeric pH Indicators: Phenolphthalein formaldehyde and o-cresol phthalein formaldehyde. *J. Polym. Sci., Part A: Polym. Chem.* **2005**, *43*, 1019–1027.
- (39) Zhao, L.; Ling, Q.; Liu, X.; Hang, C.; Zhao, Q.; Liu, F.; Gu, H. Multifunctional triazolylferrocenyl Janus dendron: Nanoparticle stabilizer, smart drug carrier and supramolecularnanoreactor. *Appl. Organomet. Chem.* **2018**, *32*, 4000–4012.
- (40) Kaiser, K.; Scriven, L. M.; Schulz, F.; Gawel, P.; Gross, L.; Anderson, H. L. Ansp-hybridized molecular carbon allotrope, cyclo [18] carbon. *Science* **2019**, *365*, 1299–1301.
- (41) Roberts, H. N.; Brown, N. J.; Edge, R.; Fitzgerald, E. C.; Ta, Y. T.; Collison, D.; Low, P. J.; Whiteley, M. W. Synthesis, redox chemistry, and electronic structure of the butadiynyl and hexatriynyl complexes [Mo{(C≡C)_nC≡CR}(L₂)(η-C₇H₇)]^{z+} (n = 1, 2; z = 0, 1; R = SiMe₃, H; L₂ = 2,2'-bipyridine, Ph₂PCH₂CH₂PPh₂). *Organometallics* **2012**, *31* (17), 6322–6335.
- (42) Woodcock, H. L.; Schaefer, H. F., III; Schreiner, P. R. Problematic energy differences between cumulenes and polyynes: does this point to a systematic improvement of density functional theory? *J. Phys. Chem. A* **2002**, *106*, 11923–11931.
- (43) Kim, J.; Swager, T. M. Control of conformational and interpolymer effects in conjugated polymers. *Nature* **2001**, *411*, 1030–1034.
- (44) Yu, M.; Shi, M.; Chen, Z.; Li, F.; Li, X.; Gao, Y.; Xu, J.; Yang, H.; Zhou, Z.; Yi, T.; Huang, C. Highly sensitive and fast responsive fluorescence turn-on chemodosimeter for Cu²⁺ and its application in live cell imaging. *Chem. - Eur. J.* **2008**, *14*, 6892–6900.
- (45) Quang, D. T.; Kim, J. S. Fluoro and chromogenic chemodosimeters for heavy metal ion detection in solution and biospecimens. *Chem. Rev.* **2010**, *110*, 6280–6301.
- (46) Ahmad, A.; Kurkina, T.; Kern, K.; Balasubramanian, K. Applications of the static quenching of rhodamine B by carbon nanotubes. *ChemPhysChem* **2009**, *10*, 2251–2255.
- (47) Yi, X. Q.; He, Y. F.; Cao, Y. S.; Shen, W. X.; Lv, Y. Y. Porphyrinic probe for fluorescence “turn-on” monitoring of Cu⁺ in aqueous buffer and mitochondria. *ACS Sens.* **2019**, *4*, 856–864.
- (48) Keizer, J. Nonlinear fluorescence quenching and the origin of positive curvature in Stern-Volmer plots. *J. Am. Chem. Soc.* **1983**, *105*, 1494–1498.
- (49) Kaneyoshi, S.; Zou, T.; Ozaki, S.; Takeuchi, R.; Udou, A.; Nakahara, T.; Fujimoto, K.; Fujii, S.; Sato, S.; Takenaka, S. Cyclic naphthalene diimide with a ferrocene moiety as a redox-active tetraplex-DNA ligand. *Chem. - Eur. J.* **2020**, *26*, 139–142.
- (50) Bhatta, S. R.; Bheemireddy, V.; Thakur, A. A redox-driven fluorescence “off-on” molecular switch based on a 1, 1'-unsymmetrically substituted ferrocenylcoumarin system: mimicking combinational logic operation. *Organometallics* **2017**, *36*, 829–838.
- (51) Alfonso, M.; Tarraga, A.; Molina, P. Ferrocenylbenzobisimidazole for recognition of anions and cations. *Inorg. Chem.* **2013**, *52*, 7487–7496.
- (52) Uliniuc, A.; Popa, M.; Drockenmuller, E.; Boisson, F.; Leonard, D.; Hamaide, T. Toward tunable amphiphilic copolymers via CuAAC click chemistry of oligocaprolactones onto starch backbone. *Carbohydr. Polym.* **2013**, *96*, 259–269.
- (53) Bhatta, S. R.; Pal, A.; Sarangi, U. K.; Thakur, A. Ferrocene appended fluorescein-based ratiometric fluorescence and electrochemical chemosensor for Fe³⁺ and Hg²⁺ ions in aqueous media: application in real samples analysis. *Inorg. Chim. Acta* **2019**, *498*, 119097–119108.
- (54) Wittke, G. Reactions of phenolphthalein at various pH values. *J. Chem. Educ.* **1983**, *60*, 239–240.
- (55) Yates, E. A.; Philipp, B.; Buckley, C.; Atkinson, S.; Chhabra, S. R.; Sockett, R. E.; Goldner, M.; Dessaux, Y.; Camara, M.; Smith, H.; Williams, P. N-Acylhomoserine lactones undergo lactonolysis in a pH-, temperature-, and acyl chain length-dependent manner during growth of *Yersinia pseudotuberculosis* and *Pseudomonas aeruginosa*. *Infect. Immun.* **2002**, *70*, 5635.
- (56) Fugit, K. D.; Anderson, B. D. The role of pH and ring-opening hydrolysis kinetics on liposomal release of topotecan. *J. Controlled Release* **2014**, *174*, 88–97.
- (57) Schäfer, A.; Huber, C.; Ahlrichs, R. Fully optimized contracted Gaussian basis sets of triple zeta valence quality for atoms Li to Kr. *J. Chem. Phys.* **1994**, *100*, 5829–5835.
- (58) Taylor, T. J.; Gabbai, F. P. Supramolecular stabilization of α,ω-diphenylpolyynes by complexation to the tridentate lewis acid [o-C₆F₄Hg]₃. *Organometallics* **2006**, *25*, 2143–2147.
- (59) Casas-Solvás, J. M.; Vargas-Berenguel, A.; Capitan-Vallvey, L. F.; Santoyo-Gonzalez, F. Convenient methods for the synthesis of ferrocene-carbohydrate conjugates. *Org. Lett.* **2004**, *6*, 3687–3690.
- (60) Frisch, M. J.; Trucks, G. W.; Schlegel, H. B.; Scuseria, G. E.; Robb, M. A.; Cheeseman, J. R.; Scalmani, G.; Barone, V.; Petersson, G. A.; Nakatsuji, H.; Li, X.; Caricato, M.; Marenich, A. V.; Bloino, J.; Janesko, B. G.; Gomperts, R.; Mennucci, B.; Hratchian, H. P.; Ortiz, J. V.; Izmaylov, A. F.; Sonnenberg, J. L.; Williams-Young, D.; Lipparini, F. D.; Egidi, F.; Goings, J.; Peng, B.; Petrone, A.; Henderson, T.; Ranasinghe, D.; Zakrzewski, V. G.; Gao, J.; Rega, N.; Zheng, G.; Liang, W.; Hada, M.; Ehara, M.; Toyota, K.; Fukuda, R.; Hasegawa, J.; Ishida, M.; Nakajima, T.; Honda, Y.; Kitao, O.; Nakai, H.; Vreven, T.; Throssell, K.; Montgomery, J. A., Jr.; Peralta, J. E.; Ogliaro, F.; Bearpark, M. J.; Heyd, J. J.; Brothers, E. N.; Kudin, K. N.; Staroverov, V. N.; Keith, T. A.; Kobayashi, R.; Normand, J.; Raghavachari, K.; Rendell, A. P.; Burant, J. C.; Iyengar, S. S.; Tomasi, J.; Cossi, M.; Millam, J. M.; Klene, M.; Adamo, C.; Cammi, R.; Ochterski, J. W.; Martin, R. L.; Morokuma, K.; Farkas, O.; Foresman, J. B.; Fox, D. J. *Gaussian 16*, Revision B.01; Gaussian, Inc.: Wallingford, CT, 2016.
- (61) (a) Becke, A. D. A new mixing of Hartree–Fock and local density-functional theories. *J. Chem. Phys.* **1993**, *98*, 1372–1377. (b) Lee, C.; Yang, W.; Parr, R. G. Development of the Colle-Salvetti correlation-energy formula into a functional of the electron density. *Phys. Rev. B: Condens. Matter Mater. Phys.* **1988**, *37*, 785–789. (c) Becke, A. D. Density-functional exchange-energy approximation with correct asymptotic behaviour. *Phys. Rev. A: At., Mol., Opt. Phys.* **1988**, *38*, 3098–3100. (d) Grimme, S.; Antony, J.; Ehrlich, S.; Krieg, H. A consistent and accurate ab initio parametrization of density functional dispersion correction (DFT-D) for the 94 elements H–Pu. *J. Chem. Phys.* **2010**, *132*, 154104–19.
- (62) (a) Klamt, A.; Schuurmann, G. COSMO: A new approach to dielectric screening in solvents with explicit expressions for the screening energy and its gradient. *J. Chem. Soc., Perkin Trans. 2* **1993**, *2*, 799–805. (b) Barone, V.; Cossi, M. Quantum calculation of molecular energies and energy gradients in solution by a conductor solvent model. *J. Phys. Chem. A* **1998**, *102*, 1995–2001.
- (63) (a) Glendening, E. D.; Reed, A. E.; Carpenter, J. E.; Weinhold, F. NBO, version 3.1; University of Wisconsin: Madison, WI, 2001. (b) Reed, A. E.; Curtiss, L. A.; Weinhold, F. Intermolecular interactions from a natural bond orbital, donor-acceptor viewpoint. *Chem. Rev.* **1988**, *88*, 899–926.
- (64) Wiberg, K. B. Application of the pople-santry-segal CNDO method to the cyclopropylcarbinyl and cyclobutylcation and to bicyclobutane. *Tetrahedron* **1968**, *24*, 1083–1096.
- (65) Andrienko, G. A. <http://www.chemcraftprog.com>.